

# Theoretical Studies on the Electronic Properties of $R_2M_{14}B$ ( $R$ = Lanthanides from La to Lu; $M$ = Mn, Fe, Co, and Ni)<sup>①</sup>

RAO Shuang<sup>a, b</sup>    LIN Chen-Sheng<sup>a, c</sup>

HE Zhang-Zhen<sup>a</sup>    CHAI Guo-Liang<sup>a②</sup>

<sup>a</sup> (State Key Laboratory of Structural Chemistry, Fujian Institute of Research on the Structure of Matter, Chinese Academy of Sciences (CAS), Fuzhou 350002, China)

<sup>b</sup> (College of Chemistry, Fuzhou University, Fuzhou 350108, China)

<sup>c</sup> (Fujian Provincial Key Laboratory of Theoretical and Computational Chemistry, Xiamen 361005, China)

**ABSTRACT** To search for an alternative for  $Nd_2Fe_{14}B$ , we have studied the electronic structures of  $R_2M_{14}B$  compounds, where  $R$  stands for rare-earth element and  $M$  for Mn, Fe, Co and Ni. By density functional theory (DFT), we discuss the atomic coordination environment and partial density of states (PDOS) in detail, with the emphasis on the interaction between the six kinds of  $M$  sites and the  $R$  atoms. We systemically calculated the electronic structures of sixty  $R_2M_{14}B$  compounds to provide systematic and reliable results for explaining the origination of magnetism, which is important for further development of  $Nd_2Fe_{14}B$  based magnet materials.

**Keywords:** partial density of states,  $Nd_2Fe_{14}B$ , density functional theory, electronic structure;

**DOI:** 10.14102/j.cnki.0254-5861.2011-2846

## 1 INTRODUCTION

At present, the rare-earth permanent magnet materials possess excellent magnetic properties and are hard to be surpassed by other materials both in business and our daily life. They are widely applied in various kinds of electronic products, automobile parts manufacturing, frequency conversion household appliances and other fields<sup>[1]</sup>. Although  $Nd_2Fe_{14}B$  is a popular permanent magnetic material, its Curie temperature is only half of that of Fe bulk<sup>[2]</sup>. In addition, when the requirements for magnetic properties are not strict, some materials with poor behaviors can be selected as substitutes, such as  $MnAl$ ,  $Mn_2Ga$  and other manganese-based materials,  $CoFe_2O_4$ ,  $Co_2C$ ,  $CoFe_2C$  and other cobalt-based materials, as well as  $FeNi$  compounds<sup>[3]</sup>. For example,  $CoFe_2O_4$  in ferrite materials has adjustable coercivity, large magneto-crystalline anisotropy. The saturation magnetization increases with the increasing temperature, which makes it occupy a unique position in magnetic materials<sup>[4]</sup>. Generally, two criteria for

evaluating the magnetic properties of  $Nd_2Fe_{14}B$  are large saturation magnetization and magneto-crystalline anisotropy energy<sup>[5]</sup>. Replacing the three constituent elements ( $Nd$ ,  $Fe$ ,  $B$ ) with other elements or doped by other elements can effectively improve its performance. Investigation of the electronic structures of  $Nd_2Fe_{14}B$  and its related structures is important for explaining the magnetization and magneto-crystalline anisotropy for further development of  $Nd_2Fe_{14}B$  based magnet materials and the origination of magnetism.

It is well known that in  $Nd_2Fe_{14}B$  the saturation magnetization and magneto-crystalline anisotropy energy depend on  $Fe$  and  $Nd$ , respectively<sup>[6, 7]</sup>. Apart from that, the  $B$  element is the main one to stabilize the configuration of this ternary compound. There are six kinds of nonequivalent sites for  $Fe$  in  $Nd_2Fe_{14}B$ , named  $Fe(4e)$ ,  $Fe(4c)$ ,  $Fe(8j1)$ ,  $Fe(8j2)$ ,  $Fe(16k1)$  and  $Fe(16k2)$ , respectively<sup>[8, 9]</sup>. In  $Nd_2Fe_{14}B$ , when  $Fe$  atoms are replaced by  $Co$  or  $Ni$ , they prefer to occupy the  $k1$  site, which enhances the  $Nd-M$  interaction and Curie temperature<sup>[10-13]</sup>. When  $Fe$  atoms are replaced by  $Mn$ , the  $j2$

Received 13 April 2020; accepted 19 May 2020

① This project was supported by the National Natural Science Foundation of China (No. 21703248), the Strategic Priority Research Program of the Chinese Academy of Sciences (No. XDB20000000), and the STS program under cooperative agreement between Fujian Province and Chinese Academy of Sciences (No. 2017T3004)

② Corresponding author. Chai Guo-Liang. E-mail: g.chai@fjirsm.ac.cn

site is the preference with the result that diminishes the Nd–M interaction and Curie temperature. Some previous experimental and theoretical researches studied several structures of doped Nd<sub>2</sub>Fe<sub>14</sub>B. However, there has been no systemic studies focusing on all the possible R<sub>2</sub>M<sub>14</sub>B (R = lanthanides from La to Lu; M = Mn, Fe, Co, and Ni) structures. In this paper, we systematically studied the electronic properties of all the sixty R<sub>2</sub>M<sub>14</sub>B compounds. The crystal structures and magnetic mechanisms of R<sub>2</sub>M<sub>14</sub>B are further explained by the partial density of states (PDOS). This work provides systemic electronic structure results for future development of alternatives to Nd<sub>2</sub>Fe<sub>14</sub>B.

## 2 COMPUTATIONAL DETAILS

The magnetic mechanisms of  $R_2M_{14}B$  ( $R$  = lanthanides from La to Lu;  $M$  = Mn, Fe, Co, and Ni) were studied in the framework of density functional theory (DFT)<sup>[14]</sup>. These calculations were performed using Vienna *ab-initio* Simulation Package (VASP) code<sup>[15]</sup>. The cutoff energy was set to 400 eV and the exchange correlation with the generalized gradient approximation (GGA)<sup>[16]</sup>, given by Perdew-Burke-Ernzerhof (PBE) was used<sup>[17]</sup>. A  $6 \times 6 \times 4$   $k$ -point mesh of the Monkhorst-Pack sampling in the Brillouin zone was chosen.

When calculating the total magnetic moment, the spin-orbital coupling is considered both for the rare-earth elements and transition metal elements. There are four formula units in

a supercell of each  $\text{R}_2\text{M}_{14}\text{B}$  cell with 68 atoms in total. The local magnetic moment of a single atom can be used to analyze the chemical environment (bond length, bond angle, bond energy, etc.), which is helpful to understand the interaction between each two atoms. The partial density of states (PDOS) of atoms in compounds is used to analyze the number of occupied states of electrons and the bonding ability. It is of great significance to characterize the electronic properties of  $\text{R}_2\text{M}_{14}\text{B}$  by PDOS<sup>[18]</sup> to analyze the origination of magnetism.

### 3 RESULTS AND DISCUSSION

### 3.1 Geometry and electronic structure of Nd<sub>2</sub>Fe<sub>14</sub>B

The optimized lattice constants of  $\text{Nd}_2\text{Fe}_{14}\text{B}$  crystal are  $a = b = 8.7518 \text{ \AA}$  and  $c = 12.1082 \text{ \AA}$  with space group of  $P4_2/mnm$ . There are 56 Fe atoms in the unit cell of  $\text{Nd}_2\text{Fe}_{14}\text{B}$ , which can be divided into six kinds of unequal Fe atoms in crystallography. Some different characters of the six kinds of Fe sites are listed in Table 1. The coordination environment of these Fe atoms is shown in Fig. 1, including surrounding atoms and bond lengths. It can be seen from Table 1 that the order of local magnetic moment is  $\text{Fe}(8j2) > \text{Fe}(4c) > \text{Fe}(16k2) > \text{Fe}(16k1) = \text{Fe}(8j1) > \text{Fe}(4e)$ , which is consistent with the experimental results<sup>[8]</sup>. This indicates that our calculation method is reliable. Therefore, we use this method to deal with  $\text{R}_2\text{M}_{14}\text{B}$  ( $\text{R} = \text{La} \sim \text{Lu}$ ,  $\text{M} = \text{Fe}, \text{Co}, \text{Ni}, \text{Mn}$ ) compounds to obtain the electronic structure information.

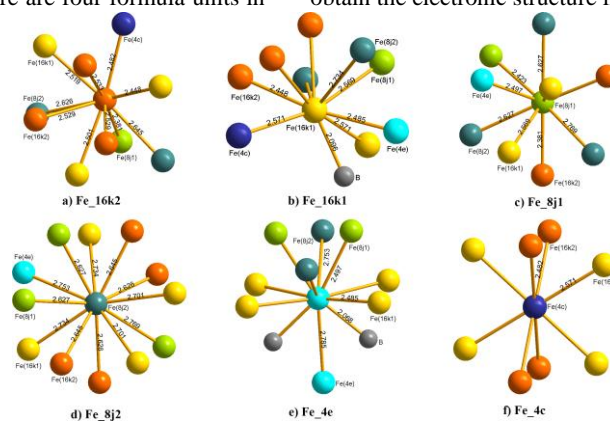


**Fig. 1. Coordination atoms of six kinds of Fe sites in Nd<sub>2</sub>Fe<sub>14</sub>B.**

**Table 1. Coordination Conditions of Six Kinds of Fe Sites in Nd<sub>2</sub>Fe<sub>14</sub>B**

Fe site of Nd <sub>2</sub> Fe <sub>14</sub> B	Fe(16 <i>k</i> 2)	Fe(16 <i>k</i> 1)	Fe(8 <i>j</i> 1)	Fe(8 <i>j</i> 2)	Fe(4 <i>e</i> )	Fe(4 <i>c</i> )
Extp. [9] (mag/μ <sub>B</sub> )	2.60	2.60	2.30	2.85	2.10	2.75
This work (mag/μ <sub>B</sub> )	2.31	2.23	2.23	2.69	2.02	2.43
Coordination numbers	10	9	9	12	9	8
Max Fe-Fe bond length/Å	2.645	2.734	2.769	2.753	2.785	2.571
Min Fe-Fe bond length/Å	2.381	2.448	2.381	2.626	2.485	2.482

The attractive and repulsive forces produced by the interaction between atoms are equal at their equilibrium bond length. When two spherical neutral atoms overlap, their orbitals are deformed. And then the outmost orbitals interact with each other and form chemical bonds, which is the manifestation of attractive force between atoms. The repulsion force includes Pauli repulsion, relative nuclear shielding, quenching of spin orbital coupling and Darwinian correction<sup>[19]</sup>. The coordination environment of these six different Fe atoms in Nd<sub>2</sub>Fe<sub>14</sub>B is shown in Fig. 1. The bond lengths of such Fe–Fe vary from 2.381 to 2.785 Å. There are four types of coordination numbers of Fe, as 8, 9, 10 and 12. The differences of the six kinds of Fe sites in Fig. 1 are shown in Table 1 with coordination number together with the nearest neighbor maximum and minimum bond length. Combining Table 1 with Fig. 1, it can be found that the dependence of local magnetic moment on coordination environment near the atom is very weak, with no obvious positive or negative correlation function relationship<sup>[20]</sup>.

Among the six kinds of Fe atoms of Nd<sub>2</sub>Fe<sub>14</sub>B, the Fe(8j2) bonds with other four kinds of Fe sites (*k1*, *k2*, *j1* and *e*). There are 12 neighbouring Fe atoms around the Fe(8j2) site. The Fe(8j2) site is surrounded by an iron network, so that its magnetic moment is enhanced. Fe(4*e*) binds to three Fe sites (*k1*, *k2*, *j1*) and one B(4*g*). It is possible that the magnetic moment of Fe(4*e*) is suppressed because of the existence of non-magnetic B atom and the hybridization between Fe and B atoms. There is also a B atom around Fe(16*k1*), but the B atom of Fe(16*k1*) is one less than that of Fe(4*e*), so the magnetic moments of these two Fe atoms are smaller. The nearest neighbour atoms of Fe(16*k2*) and Fe(16*k1*) are all 10, but the former is 10 Fe atoms, and the latter is 9 Fe and one B atoms. That is to say, the existence of this B atom makes the magnetic moment of Fe(16*k1*) smaller than that of Fe(16*k2*). As far as the bond length is concerned, compared with the bond length at the Fe(8j2) site, there may be a strong hybridization between Fe(4*e*) and B, which makes the bond length between Fe(4*e*) and B decrease<sup>[21]</sup>. Therefore, the magnetic moment at the *e* site is weakened with the decrease of bond length. On the other hand, due to the weak hybridization between Fe(8j2) and its adjacent atoms, the bond length between Fe(8j2) and its adjacent atoms becomes longer, which may result in the magnetic moment similar to that of body-centred-cubic Fe crystal<sup>[5]</sup>. In a word, there are many factors that affect the magnetic moment, such as the spatial configuration of the Fe atom, the total number of the

nearest Fe atoms and the bonding type. From the perspective of element substitution, Fe(8j2) site has the maximum magnetic moment and also occupies the largest space. The magnetic moment of Fe(4*e*) site is the smallest and occupies the smallest space. If smaller atoms replace the Fe(8j2) site, the crystal volume will reduce and the magnetic moment will change. If larger atoms enter the Fe(4*e*) site, the crystal volume will expand<sup>[11, 22]</sup>.

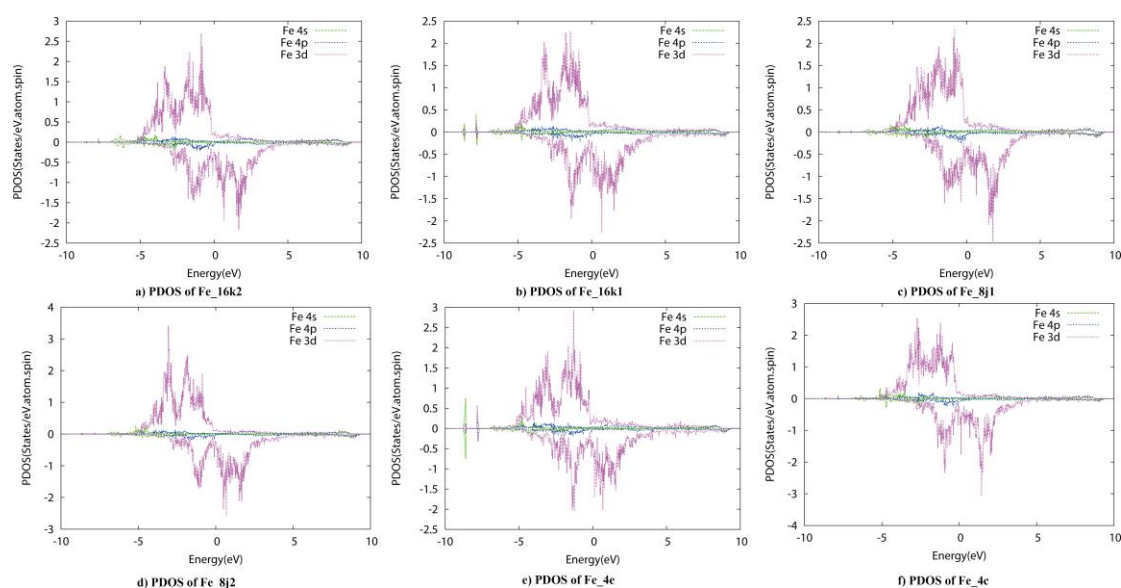
Fig. 2 shows spin-polarized partial density of state (PDOS) information of the six kinds of Fe sites of Nd<sub>2</sub>Fe<sub>14</sub>B. It can be seen from the external contour of these six kinds of Fe atoms that the 3*d* electrons play an important role. Moreover, the 3*d* electrons of these six kinds of Fe atoms occupy almost the same energy range, mainly from –5 to 5 eV, which is consistent with reference<sup>[23]</sup>. The up-spin (or majority-spin) is almost fully occupied. The down-spin (or minority-spin) is partially occupied. It can be seen that in b) and e) of Fig. 2, there are slightly small peaks from –10 to –5 eV, which corresponds to the peaks of partial density of states of B atom. It proves that there is a B atom in the nearest neighbour coordination environment of Fe(16*k1*) and Fe(4*e*) in Fig. 1. There is none Fe(4*e*) around Fe(16*k2*) but one around Fe(16*k1*). The covalency of the chemical bond around Fe(16*k2*) is weak, resulting in the 0~2 eV energy splitting in the Fe(16*k2*) PDOS in Fig. 2. Fe(4*c*) is located at the edge of the lattice, and Fe(4*e*) is located partially at the edge and partially inside of the lattice. This "inside" makes more types of atoms around Fe(4*e*) and the coordination environment more complex. Comparing Fe(8j1) with Fe(8j2), the type of the nearest neighbour atom of Fe(8j1) is 5 while Fe(8j2) is 4. The total number of the nearest neighbour atoms and its spatial configuration also lead to the difference of magnetic moment and PDOS between the two kinds of atoms.

Fig. 2 qualitatively describes the PDOS of the six kinds of Fe. In order to find out the differences among these six types, we calculate the band center and band width of their 3*d* electrons, including their up-spin and down-spin. Then, we list these values in Table 2 to quantitatively discuss the electronic structure information. It can be seen that for the center of 3*d* band, the down-spin electrons are about 2 eV higher than the up-spin ones, corresponding to Fig. 2 that 3*d* electrons are preferentially filled in the up-spin state where their energy is lower. The electron filling is from the place with lower to higher energy. For the up-spin band center of the 3*d* electrons of these six kinds of Fe atoms, the lowest energy is at 8j2 site. For the down-spin band center of the 3*d*

electrons, the highest energy is  $4c$  and the lowest is  $4e$ , while both up-spin and down-spin are  $4e$ .  
for the band width of  $3d$  electrons, the highest energy sites of

**Table 2. Electronic Structure Properties of Six Kinds of Fe Sites in  $\text{Nd}_2\text{Fe}_{14}\text{B}$**

Fe site	3d band center		3d band width	
	Up-spin	Down-spin	Up-spin	Down-spin
Fe(16k2)	-1.592	0.622	7.484	5.665
Fe(16k1)	-1.599	0.532	8.142	6.253
Fe(8j1)	-1.425	0.733	6.565	5.483
Fe(8j2)	-1.831	0.766	8.139	5.699
Fe(4e)	-1.575	0.367	9.081	7.159
Fe(4c)	-1.542	0.768	6.750	5.204



**Fig. 2. Partial density of states of the six kinds of Fe sites in  $\text{Nd}_2\text{Fe}_{14}\text{B}$ . Positive and negative corresponding to the up-spin and down-spin PDOS**

### 3.2 $\text{R}_2\text{Fe}_{14}\text{B}$ ( $\text{R} = \text{La} \sim \text{Lu}$ )

The electronic structures of  $\text{Nd}_2\text{Fe}_{14}\text{B}$  discussed above are useful for further tuning the performance by element replacing. According to the local magnetic moment of each Fe site explained by the surrounding environment of Fe site and PDOS, we replaced Nd with other rare-earth elements, and then got the electronic structures of the local sites of six kinds of Fe atoms in each  $\text{R}_2\text{Fe}_{14}\text{B}$  compound. We analyzed the influence of rare-earth element replacement on the magnetic moment of  $\text{R}_2\text{Fe}_{14}\text{B}$  on atomic scale. Fig. 3 shows the  $3d$  electron information of the six kinds of Fe sites of  $\text{R}_2\text{Fe}_{14}\text{B}$  series compounds, which includes the band center and band width of up-spin and down-spin PDOS. It can be seen from the figure that the lowest energy is at  $8j2$  site for the up-spin Fe- $3d$  band center, while for the down-spin one, the lowest energy is at  $4e$  site. For the band width of  $3d$  PDOS, the highest energy site in the up-spin and down-spin  $3d$  PDOS are

at the  $4e$  site.

It can be seen from the figure that with the increase of atomic number, the down-spin band center is almost flat (slightly decreased), while the trend of the other three properties is slightly increased, which may be caused by lanthanide contraction<sup>[24]</sup> and the interaction between Fe- $3d$  and R- $4f$  electrons. The number of filling electrons in  $4f$  shell increases with the increase of atomic number. According to Hund rule, the  $4f$  orbitals (up to 7) are occupied singly first, and then filled with up- and down-spin pairs of electrons. The interaction between Fe- $3d$  and R- $4f$  is different due to the different filling electron number and different filling orbitals, which results in the trend change of these curves. When the rare-earth element R is La or Gd, the PDOS shows a noticeable low energy shift, which may be due to the filling number of  $4f$  shell. The arrangement of electrons in the outer electronic shell of Fe, La, and Gd atoms are  $3d^6 4s^2$ ,  $5d^1 6s^2$

and  $4f^7 5d^1 6s^2$ , respectively. The  $4f$  shell has no electron for La<sup>[25]</sup>, but it is half-filled for Gd<sup>[26]</sup>. The band width of Fe- $3d$  occupied state of most R<sub>2</sub>Fe<sub>14</sub>B is wider than that of La<sub>2</sub>Fe<sub>14</sub>B and Gd<sub>2</sub>Fe<sub>14</sub>B. In a word, the substitution of rare-earth

elements has few effects on the R-Fe interaction and the electronic structure of R<sub>2</sub>Fe<sub>14</sub>B. Furthermore, this explains why R<sub>2</sub>Fe<sub>14</sub>B series compounds can exist stably.

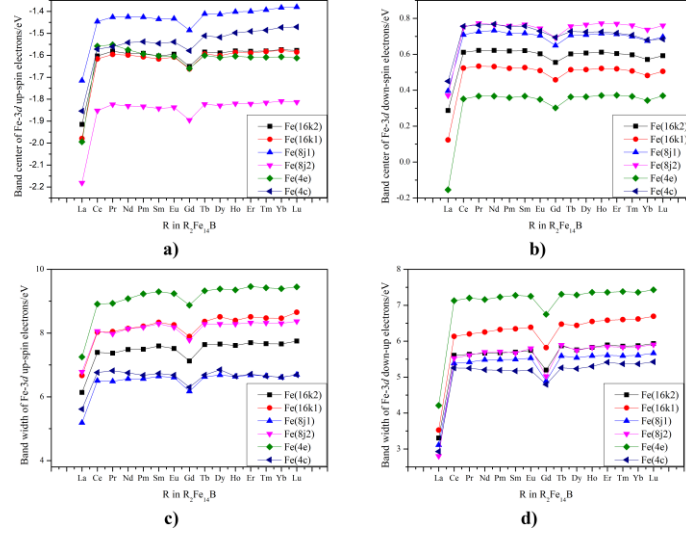


Fig. 3. Partial density of states of six kinds of Fe sites in R<sub>2</sub>Fe<sub>14</sub>B

### 3.3 R<sub>2</sub>M<sub>14</sub>B (R = La ~ Lu, M = Co, Ni, Mn)

In this section, we further discuss the electronic structure changes by replacing the M sites in R<sub>2</sub>M<sub>14</sub>B. Here, M denotes for Co, Ni, and Mn. The results are shown in Figs. 4~6. In bcc-Fe crystal, there are eight nearest neighbors around each Fe atom. The ground state is ferromagnetic configuration at a stable ferromagnetic phase<sup>[27]</sup>. The bcc-Co is a ferromagnetic phase with large magnetic moment and large spin splitting<sup>[28]</sup>. The fcc-Ni crystal shows stable ferromagnetic phase<sup>[29]</sup>. The bcc and fcc phases of Mn exist naturally only at high temperature. But the temperature is too high to have any kind of magnetic sequence. The stable room temperature phase of Mn is a complex bcc structure, each unit has 29 atoms, and it is antiferromagnetic phase at low temperature<sup>[30]</sup>. Here, bcc and fcc represent body-centered-cubic and face-centered-cubic, respectively.

It can be seen from Fig. 4 that the  $3d$  band center and width of Co are higher than that of Fe. This means that the energy of electron is higher after Co substitution, which is no longer as stable as that of Fe compound. For the up-spin band center of the  $3d$  electrons of the six kinds of Co atoms, the lowest is  $4c$ . For the down-spin band center of the  $3d$  electrons, the lowest is  $4e$ . For the band width of both up-spin and down-spin of Co- $3d$  electrons, the highest energy is  $4e$ . Co and Fe are both the group VIII elements, but the former has one more  $3d$  electron than the latter. For R<sub>2</sub>Fe<sub>14</sub>B compounds in Fig. 3, in

the up-spin band center of Fe, the lowest energy is the Fe(8j2) site, while in Fig. 4, the Co(4c) site is the lowest. Therefore, when Co is used to replace Fe, different sites may be considered. Furthermore, it should show different results with different concentration of Co. Compared with Fig. 3, it shows that the band width of Co- $4e$  site increases, which indicates that the energy range affected by the interaction between R-Co atoms may lead to "tailing" and longer range. However, the general gentle trend is still unchanged. Although the substitution of Co for Fe will bring about changes, it will not change much. So, this alternative can be considered.

Next, we will discuss the substitution of Ni for Fe in R<sub>2</sub>Fe<sub>14</sub>B (shown in Fig. 5). We have found that R<sub>2</sub>Co<sub>14</sub>B is similar to R<sub>2</sub>Fe<sub>14</sub>B, but now we can see that the electronic structure information of R<sub>2</sub>Ni<sub>14</sub>B series compounds has begun to change dramatically. As a whole, the band center and band width of the up-spin and down-spin of Ni- $3d$  orbitals are higher than those of Fe- $3d$ , and the extent of Ni- $3d$  is higher than that of Co- $3d$ . That is to say, Ni has a great influence on magnetic moment of R<sub>2</sub>Ni<sub>14</sub>B. More rigorous experimental conditions are needed when replacing Fe in R<sub>2</sub>Fe<sub>14</sub>B with Ni. Generally, the electronic structure shows differences in the band center of R<sub>2</sub>Ni<sub>14</sub>B series between light and heavy rare-earth elements. The energy of light rare-earth compound is lower than that of heavy one when considering the up-spin band center, while it is opposite for the down-spin one. It can

be seen that there are peaks or troughs when  $R = \text{Pm}$  in the up-spin and down-spin band centers. Moreover, La, Gd and Tb are also obvious turning points, which may be caused by the arrangement of  $3d^8 4s^2$  electron shell of Ni. Ni has two more  $3d$  electrons than Fe, but Fe has two more unpaired electrons than Ni. In  $R_2M_{14}B$ , the interaction between unpaired electrons of rare-earth  $R$  and  $M$  forms a bond, so the

bond of  $R\text{-Fe}$  is stronger and more thorough than that of  $R\text{-Ni}$ . Furthermore, the strong interaction between  $R\text{-}4f$  and  $M\text{-}3d$  is quite difficult in this study. In both up-spin and down-spin of the  $\text{Co-}3d$  band width, the widest band is the  $4e$  site and the narrowest one is  $8j/2$ . Therefore, when Ni replaces Fe, the substitution of  $4e$  and  $8j/2$  sites should be paid more attention.

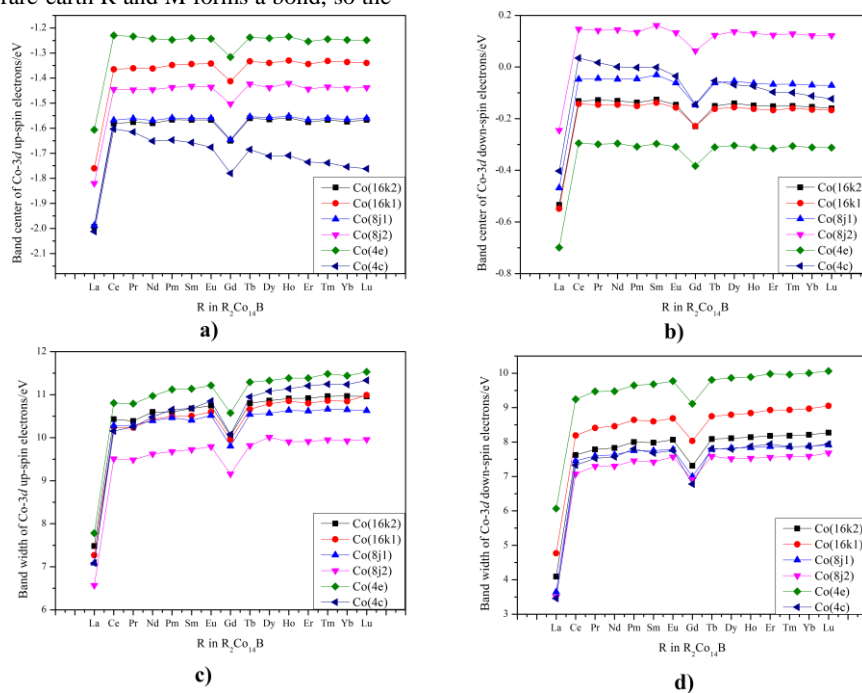


Fig. 4. Partial density of states of six kinds of Co sites in  $R_2\text{Co}_{14}\text{B}$

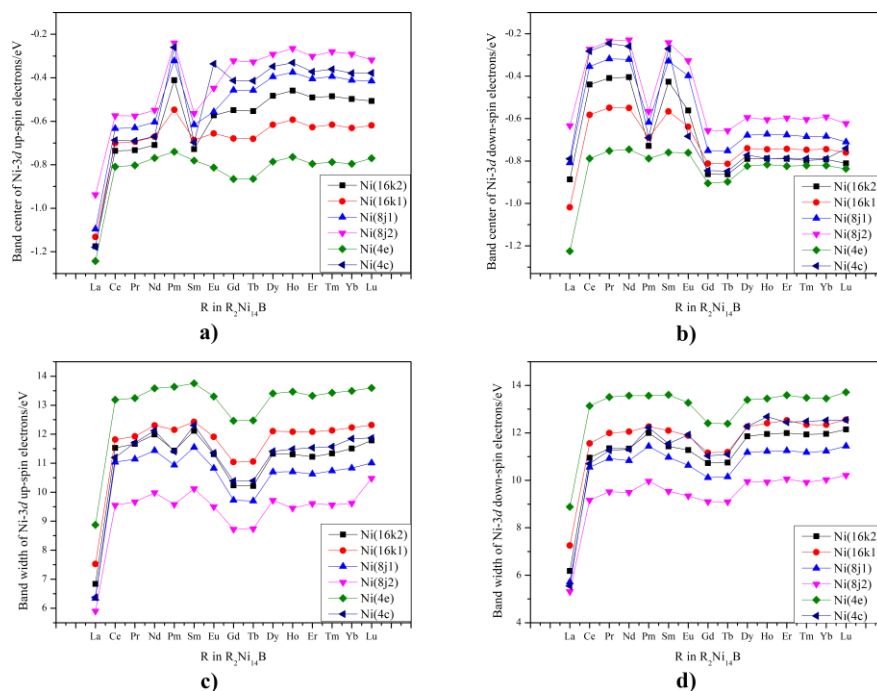


Fig. 5. Partial density of states of six kinds of Ni sites in  $R_2\text{Ni}_{14}\text{B}$

When discussing  $R_2\text{Mn}_{14}\text{B}$ , we divide rare-earth elements in Fig. 6 into two parts,  $\text{La} \sim \text{Pr}$  and  $\text{Nd} \sim \text{Lu}$ . In the latter one,

the curve is gentle and slightly downward in the band center and band width of up-spin and down-spin  $\text{Mn-}3d$  electrons,

similar to R<sub>2</sub>Fe<sub>14</sub>B, which may be due to the similar covalent radii of Mn and Fe. However, the energy of Mn(4c), Mn(4e) and Mn(8j1) in the band center of the up-spin 3d electrons is greater than 0 eV, indicating that it may be more difficult for Mn to replace these three sites in Fe. It may require sufficient energy from the outside environment. Compared with R<sub>2</sub>Fe<sub>14</sub>B, R<sub>2</sub>Mn<sub>14</sub>B has a narrower up- and down-spin band width. That is to say, the 3d electron of Mn is more localized than that of Fe, Co and Ni. Although manganese compounds possess high magnetic properties, the configuration between Mn-3d and R-4f becomes antiferromagnetic, which reduces the magnetic moment due to the fact that the 3d shell of

manganese is 3d<sup>5</sup>4s<sup>2</sup> (half-filled) and the manganese atoms in R<sub>2</sub>Mn<sub>14</sub>B are closely packed together. It was found that in experiment the manganese atoms in Er<sub>2</sub>(Fe, Mn)<sub>14</sub>B tend to be at the j1 and j2 sites, while the Fe atoms tend to be at the k1 and k2 sites. This is different with our theoretical researches as many factors such as electronegativity, valence electron number or crystal field may also be important<sup>[22]</sup>. We found that Gd in R<sub>2</sub>Mn<sub>14</sub>B is no longer as special as Gd compounds in the previous three transition metals. That is to say, in R<sub>2</sub>Mn<sub>14</sub>B, the main influence is not rare-earth R but Mn, which is similar to R<sub>2</sub>Ni<sub>14</sub>B.

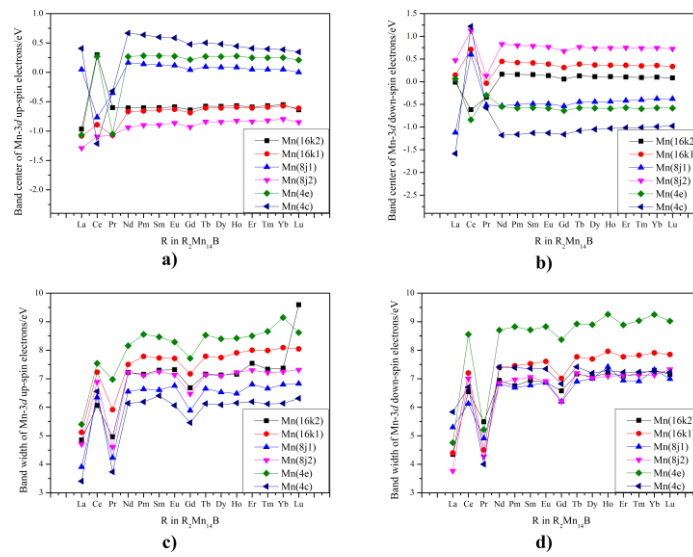


Fig. 6. Partial density of states of six kinds of Mn sites in R<sub>2</sub>Mn<sub>14</sub>B

#### 4 CONCLUSION

In order to find new rare-earth permanent magnetic materials, we have studied the replacement of rare-earth element Nd and transition metal element Fe of Nd<sub>2</sub>Fe<sub>14</sub>B by density functional theory. We analyzed the electronic structures of R<sub>2</sub>M<sub>14</sub>B compounds, in which R represents rare-earth element from La to Lu and M represents transition metal such as Mn, Fe, Co and Ni. We found that the order of local magnetic moment of Fe in Nd<sub>2</sub>Fe<sub>14</sub>B is Fe(8j2) > Fe(4c) > Fe(16k2) > Fe(16k1) = Fe(8j1) > Fe(4e). The maximum and minimum may be related to the coordination environment, coordination number and coordination atom type of Fe atom. Corresponding to the six kinds of Fe-3d electron information in PDOS, the lowest energy of 3d electron up-spin band center is at 8j2 site, and the lowest energy of down-spin band center is 4e. For the 3d band width, the highest energy site of the up- and down-spin electrons is

4e. When rare-earth elements are substituted, the results are the same as those in Nd<sub>2</sub>Fe<sub>14</sub>B, that is to say, rare-earth substitution has few effects on the Fe series compounds. With the change of rare-earth elements in each site, the general trend is due to the contraction of lanthanides. When the transition metal element Fe is substituted by Co, the energy of the up- and down-spin of Co-3d electrons is higher, indicating the stability of the compound is decreasing. The band width of Co-4e site is larger than that of Fe-4e, showing that the energy range of the interaction between R-Co atoms may be longer. However, the general trend changes little, which illustrates that the substitution of Co for Fe can be considered. When the transition metal element Fe is substituted by Ni, the band center and band width of Ni-3d electrons are higher even than those of Co-3d. That is to say, Ni has a great influence on the magnetic moment. There are differences in the band center diagram of R<sub>2</sub>Ni<sub>14</sub>B series between light and heavy rare-earth elements. It may be because Fe has two more unpaired



electrons than Ni, so the bonding of R-Fe in  $R_2Fe_{14}B$  is stronger and the interaction is more thorough than that of R-Ni in  $R_2Ni_{14}B$ . When  $R_2Mn_{14}B$  is discussed, in Nd~Lu, the band center and band width of Mn-3d electrons are generally similar to  $R_2Fe_{14}B$ , which may be due to the similar covalent radii of Mn and Fe. Compared with  $R_2Fe_{14}B$ ,  $R_2Mn_{14}B$  has a narrower band width, which may be that the Mn-3d electrons are more localized than that of Fe, Co and Ni. Although manganese compounds display high magnetic properties, the Mn-3d shell is half fulfilled and Mn atoms in  $R_2Mn_{14}B$  are

closely arranged together. Therefore, the magnetic configuration between Mn-3d and R-4f becomes antiferromagnetic, which reduces the magnetic moment. That is to say, in  $R_2Mn_{14}B$ , the main factor is not rare-earth R but Mn, just like  $R_2Ni_{14}B$  series.

In our systematic substitution study, we analyzed the electronic structure properties of transition metal sites of  $R_2M_{14}B$  series compounds, discussed the possibility and reasonability of the existence of substituted compounds, and finally clarified the origination of magnetism.

## REFERENCES

- (1) Sagawa, M.; Fujimura, S.; Togawa, N.; Yamamoto, H.; Matsuura, Y. New material for permanent magnets on a base of Nd and Fe. *J. Appl. Phys.* **1984**, 55, 2083–2087.
- (2) Croat, J. J.; Herbst, J. F.; Lee, R. W.; Pinkerton, F. E. Pr-Fe and Nd-Fe-based materials: a new class of high-performance permanent magnets. *J. Appl. Phys.* **1984**, 55, 2078–2082.
- (3) Skomski, R.; Coey, J. M. D. Magnetic anisotropy - how much is enough for a permanent magnet? *Scripta. Mater.* **2015**, 112, 3–8.
- (4) Jia, Z.; Ren, D.; Zhu, R. Synthesis, characterization and magnetic properties of  $CoFe_2O_4$  nanorods. *Mater. Lett.* **2012**, 66, 128–131.
- (5) Khan, I.; Hong, J. Electronic structure and magnetic properties of  $Nd_2Fe_{14}B$ . *J. Korean Phys. Soc.* **2016**, 68, 1409–1414.
- (6) Bolzoni, F.; Moze, O.; Pareti, L. First-order field-induced magnetization transitions in single-crystal  $Nd_2Fe_{14}B$ . *J. Appl. Phys.* **1987**, 62, 615–620.
- (7) Yamada, O.; Tokuhara, H.; Ono, F.; Sagawa, M.; Matsuura, Y. Magnetocrystalline anisotropy in  $Nd_2Fe_{14}B$  intermetallic compound. *J. Magn. Magn. Mater.* **1986**, 54, 585–586.
- (8) Givord, D.; Li, H. S.; Tasset, F. Polarized neutron study of the compounds  $Y_2Fe_{14}B$  and  $Nd_2Fe_{14}B$ . *J. Appl. Phys.* **1985**, 57, 4100–4102.
- (9) Ching, W. Y.; Gu, Z. Q. Electronic structure of  $Nd_2Fe_{14}B$ . *J. Appl. Phys.* **1987**, 61, 3718–3720.
- (10) Abache, C.; Oesterreicher, H. Structural and magnetic properties of  $R_2Fe_{14-x}T_xB$  (R = Nd, Y; T = Cr, Mn, Co, Ni, Al). *J. Appl. Phys.* **1986**, 60, 1114–1117.
- (11) Bolzoni, F.; Leccabue, F.; Moze, O.; Pareti, L.; Solzi, M. Magnetocrystalline anisotropy of Ni and Mn substituted  $Nd_2Fe_{14}B$  compounds. *J. Magn. Magn. Mater.* **1987**, 67, 373–377.
- (12) Doi, M.; Matsui, M. Substitution effect of Fe sites in  $Nd_2Fe_{14}B$ . *IEEE Translat. J. Magn. Jpn.* **1992**, 7, 38–44.
- (13) Wang, H. Y.; Zhao, F. A.; Chen, N. X.; Liu, G. Theoretical investigation on the phase stability of  $Nd_2Fe_{14}B$  and site preference of V, Cr, Mn, Zr and Nb. *J. Magn. Magn. Mater.* **2005**, 295, 219–229.
- (14) Runge, E.; Gross, E. K. U. Density-functional theory for time-dependent systems. *Phys. Rev. Lett.* **1984**, 52, 997–1000.
- (15) Reinhard, M.; Giehl, K.; Abel, K.; Haffner, C.; Jarchau, T.; Hoppe, V.; Jockusch, B. M.; Walter, U. The proline-rich focal adhesion and microfilament protein VASP is a ligand for profilins. *EMBO. J.* **1995**, 14, 1583–1589.
- (16) Miyake, T.; Akai, H. Quantum theory of rare-earth magnets. *J. Phys. Soc. Jpn.* **2018**, 87, 041009–10.
- (17) Maintz, S.; Deringer, V. L.; Tchougréff, A. L.; Dronskowski, R. Analytic projection from plane-wave and PAW wavefunctions and application to chemical-bonding analysis in solids. *J. Comput. Chem.* **2013**, 34, 2557–2567.
- (18) Wolfram, T.; Elliatiglu, S. Density-of-states and partial-density-of-states functions for the cubic d-band perovskites. *Phys. Rev. B* **1982**, 25, 2697–2714.
- (19) Wang, S. G.; Schwarz, W. H. E. Lanthanide diatomics and lanthanide contractions. *J. Phys. Chem. C* **1995**, 99, 11687–11695.
- (20) James, P.; Eriksson, O.; Johansson, B.; Abrikosov, I. A. Calculated magnetic properties of binary alloys between Fe, Co, Ni, and Cu. *Phys. Rev. B* **1999**, 59, 419–430.
- (21) Kitagawa, I. Calculation of electronic structures and magnetic moments of  $Nd_2Fe_{14}B$  and  $Dy_2Fe_{14}B$  by using linear-combination-of-pseudo-atomic-orbital method. *J. Appl. Phys.* **2009**, 105, 07E502–3.
- (22) Fuerst, C. D.; Meisner, G. P.; Pinkerton, F. E.; Yelon, W. B. Site occupancy in erbium-iron-manganese-boron alloys. *J. Less Common. Met.* **1987**, 133, 255–261.



- (23) Jaswal, S. S.; Langell, M. A.; Ren, Y. G.; Engelhardt, M. A.; Sellmyer, D. J. Electronic structure and surface reactivity of  $Nd_2Fe_{14}B$  and related compounds. *J. Appl. Phys.* **1988**, 64, 5577–5579.
- (24) Hughes, I. D.; Däne, M.; Ernst, A.; Hergert, W.; Lüders, W.; Poulter, J.; Staunton, J. B.; Svane, A.; Szotek, Z.; Temmerman, W. M. Lanthanide contraction and magnetism in the heavy rare earth elements. *Nature* **2007**, 446, 650–653.
- (25) Maple, M. B.; Witting, J.; Kim, K. S. Pressure-induced magnetic-nonmagnetic transtion of Ce impurities in La. *Phys. Rev. Lett.* **1969**, 23, 1375–1377.
- (26) Kitagawa, I.; Asari, Y. Magnetic anisotropy of  $R_2Fe_{14}B$  ( $R$  = Nd, Gd, Y): density functional calculation by using the linear combination of pseudo-atomic-orbital method. *Phys. Rev. B* **2010**, 81, 214408–7.
- (27) Wang, C. S.; Klein, B. M.; Krakauer, H. Theory of magnetic and structural ordering in iron. *Phys. Rev. Lett.* **1985**, 54, 1852–1855.
- (28) Marcus, P. M.; Moruzzi, V. L. Equilibrium properties of the cubic phases of cobalt. *Solid State Commun.* **1985**, 55, 971–975.
- (29) Basch, H.; Newton, M. D.; Moskowitz, J. W. The electronic structure of small nickel atom clusters. *J. Chem. Phys.* **1980**, 73, 4492–4510.
- (30) Fuster, G.; Brener, N. E.; Callaway, J.; Fry, J. L.; Zhao, Y. Z.; Papaconstantopoulos, D. A. Magnetism in bcc and fcc manganese. *Phys. Rev. B* **1988**, 38, 423–432.